

Molecular Dynamics Simulation Study of the Ionic Mobility of OH⁻ Using the OSS2 Model

Song Hi Lee

Department of Chemistry, Kyungsoong University, Busan 608-736, Korea. E-mail: shlee@ks.ac.kr

Received May 9, 2006

Anomalously high ionic mobilities of H⁺ and OH⁻ are owing to the transfer of H⁺ by the Grotthus chain mechanism. Molecular dynamics simulations for the system of 215 water including OH⁻ ion at 298.15 K using the OSS2 model [*J. Chem. Phys.* **109**, 5547 (1998)] as a dissociable water model with the use of Ewald summation were carried out in order to study the dynamics of OH⁻ in water. The calculated ionic mobility of OH⁻ is in good agreement with the experimental result and the Grotthus chain mechanism is fully understood.

Key Words : Molecular dynamics simulation, OSS2 potential, Ionic mobility of OH⁻, Grotthus chain mechanism.

Introduction

Two experimental results^{1,2} of limiting equivalent conductances of electrolytes as a function of water density in supercritical water showed two different trends: Wood *et al.*¹ reported a clear change of slope from the assumed linear dependence of limiting equivalent conductances of LiCl, NaCl, NaBr, and CsBr on water density, and the other was a clear maximum in limiting equivalent conductances of NaOH reported by Ho and Palmer.² Assuming the simple additivity of limiting equivalent conductances of electrolytes from each of the component ions and eliminating the limiting equivalent conductance of Na⁺ from those of NaCl and NaOH, the limiting equivalent conductances of Cl⁻ and OH⁻ ions as a function of water density in supercritical and ambient water are compared in Figure 1. If one considers only the size effect of ion on the ionic mobility, it is expected that the limiting equivalent conductance of Cl⁻ ion is greater than that of OH⁻ since the ionic size of OH⁻ is comparable to that of F⁻ and the limiting molar conductances Cl⁻ and F⁻ at ambient water are 76 and 55 S·cm²/mol, respectively. The limiting equivalent conductances of Cl⁻ and OH⁻ ions at water density of 0.22 g/cc in Figure 1 reflects this size effect. As water density increases, the limiting equivalent conductances of Cl⁻ increases and decreases after 0.31 g/cc while that of OH⁻ increases continually, they cross each other at 0.48 g/cc, and finally in ambient water the limiting equivalent conductances of OH⁻ is much greater than that of Cl⁻.

Figure 1 suggests a significant water density effect on the ionic mobility of OH⁻. The usual behavior of the limiting equivalent conductance of Cl⁻ as a function of water density is fully understood by our previous MD simulation studies^{3,4}: the effect of the number of hydration water molecules around ions dominates in the higher-density region while the interaction between the ions and the hydration water molecules dominates in the lower-density region, and as water density increases, the large number of hydration water molecules restricts the ionic mobility of Cl⁻. However, the

limiting equivalent conductance of OH⁻ increases continually up to water density of 0.61 g/cc and then decreases. This is closely related to the well-known Grotthus chain mechanism.

The large difference of the limiting molar conductances between H⁺ and other monovalent cations in ambient water is also found in those between OH⁻ and other monovalent anions. The transport of H⁺ in water is well-known as the Grotthus chain mechanism that does not involve its actual motion through the solution. Instead of a single, highly solvated proton moving through the solution, it is believed that there is an effective motion of a proton which involves the rearrangement of bonds through a long chain of water molecules as shown Figure 2(a). A closer insight into the transport of OH⁻ reveals that the large value of the limiting molar conductance of OH⁻ is also related to the Grotthus chain mechanism as shown Figure 2(b) in addition to its actual motion through the solution.

Very recently Tuckerman *et al.*⁵ reported three different scenarios of OH⁻(aq) structural diffusion by *ab initio* molecular dynamics (AIMD) simulations using three popular density functionals, PW91, BLYP, and HCTH/120.⁶⁻⁸ They denoted the OH⁻ charge defect as (O⁺H)⁻ and the hydrogen-bonded H to O⁺ as H⁺. In the solvation pattern of OH⁻ predicted by

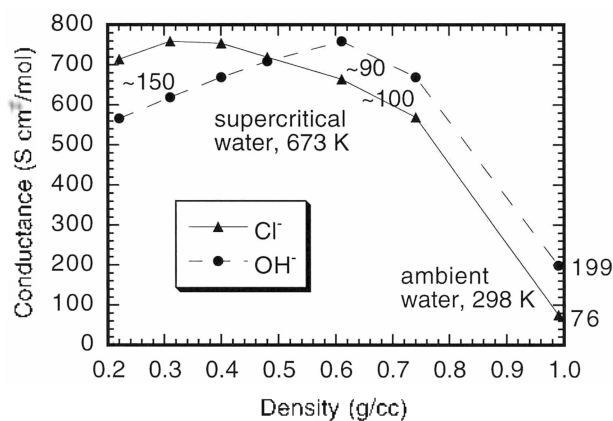


Figure 1. Limiting equivalent conductances of Cl⁻ and OH⁻ ions as a function of water density in supercritical and ambient water

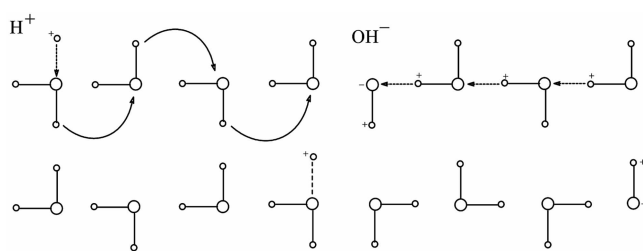


Figure 2. Grothus chain mechanisms.

PW91, the OH⁻ strongly favors three accepted hydrogen bonds (HBs) by O^{*} in addition to a fourth one by H^{*}. In this tetrahedral configuration, a neighboring water molecule can readily transfer a proton to OH⁻ upon a suitable fluctuation and thereby exchange O^{*} and H^{*}.

The solvation pattern of OH⁻ captured by BLYP predicts a mechanism that can account for the dynamical solvation shell changes from the resting state (four accepted and no donated HB) to the active state (three accepted and one donated HB), in which a proton from a neighboring water molecule can transfer to OH⁻. After this proton transfer (PT) step, the charge defect has migrated along a HB and is located, in a 4-fold coordinated state, at a neighboring vertex site. Then it relaxes to the initial resting state configuration.

In the HCTH trajectory, OH⁻ almost always accepts four HBs in addition to donating one, leading to a saturated solvation shell. Contrary to the PW91 case, here OH⁻ is rarely solvated in such a way as to receive an additional proton, thereby preventing OH⁻ from accessing a solvation pattern that allows for PT. Hence diffusion occurs primarily by the vehicle or hydrodynamic mechanism where a rather long-lived aggregate, [OH (H₂O)_n], is moving akin to simple ions such as Na⁺(aq) or Cl⁻(aq), PT and structural diffusion becoming rare events.

The aims of this paper is to determine the most possible viewpoint on the ionic mobility of OH⁻ at ambient water by employing the OSS2 model which was used to study the dissociation and reassociation of H⁺ in bulk water. In Section II, we present the molecular models and MD simulation method. We discuss our simulation results in Section III and present the concluding remarks in Section IV.

OSS2 Model

In order to study the dynamics of OH⁻ in water, it is essential to have models capable of describing how water solvent molecules can participate in ionic chemistry through dissociation and reassociation of H⁺ in OH⁻, H₂O, and H₃O⁺. Several attempts at dissociating water potentials have been made in the past, beginning with the work of Stillinger, David and Weber.⁹ Recently Ojame, Shavitt, and Singer reported progress in the design of a family of potentials for describing H⁺(H₂O)_n, called OSS(Ojame-Shavitt-Singer)_m (m = 1-3).^{10,11}

The OSS2 model has been chosen for the preliminary molecular dynamics (MD) of the solvated proton in ambient

water. It is reported that the best results were obtained using the OSS3 potential and that the OSS2 model potential also gave good results, but usually exhibited too large bond angles for water molecule.¹⁰ When that deficiency was not a serious problem for the application at hand, the OSS2 model was a preferred choice for simulation studies, because of the faster and less elaborate computer-code implementation as compared to the OSS3 model, which contains a dipole-three-body coupling term which depends both on the induced dipole moment and the geometry.

The induced dipole moment μ_i at each oxygen site in the OSS2 model can be obtained self-consistently by imposing the conditions $dV_{el}/d\mu_k = 0$ ($k = 1, 2, \dots, n_O$):¹⁰

$$\mu_i = \alpha \left[\sum_{j,j \neq i} \frac{n_H r_{ij} q}{r_{ij}^3} S_{ij}^{cd}(r_{ij}) + \sum_{j,j \neq i} \frac{T_{ij} \cdot \mu_j}{r_{ij}^3} S_{ij}^{dd}(r_{ij}) \right], \quad (1)$$

where V_{el} is the electrostatic energy, n_O and n_H are the numbers of oxygen and hydrogen atoms, α is the polarizability of the induced dipole moment, and $S_{ij}^{cd}(r_{ij})$ and $S_{ij}^{dd}(r_{ij})$ are the electric field cutoff functions for charge-dipole and dipole-dipole interactions, respectively. This method to calculate the induced dipole moment at each oxygen site is exactly the same as that used in our previous MD simulation study for Li⁺ in water¹² using the revised polarized (RPOL) model^{13,14} for Li⁺ and water with the use of Ewald summation.^{15,16} The double summation for particles i and j in the reciprocal-space cannot be reduced to one summation due to the electric field cutoff functions. We do not apply the Ewald summation in the reciprocal-space and this is reasonable since the electric field cutoff functions are for short ranged interactions and the distances dealing in the reciprocal-space are larger than the length of the simulation box. Ojame *et al.*, however, used a different method¹⁷ for the Ewald summation in the calculation of the induced dipole moment.

A canonical ensemble of fixed N (number of particles), V (volume), and T (temperature) is chosen for the simulation ensemble. The system is composed of 215 water molecules and an OH⁻ ion. Gauss's principle of least constraint¹⁸ is used to maintain the system at a constant temperature. The ordinary periodic boundary condition in the x-, y-, and z-direction and Gear's fifth order predictor-corrector method¹⁹ is used to solve the equations of motion with a time step of 2×10^{-16} second (0.2 fs).

Results and Discussion

First, the validity of the use of Ewald summation for the induced dipole moment at each oxygen site in the OSS2 model has been checked for various systems. The OSS2 model is examined for H₂O, H₃O⁺, H₃O₂⁺, H₇O₃⁺, and H₉O₄⁺. The equilibrium molecular geometries and energies obtained from molecular dynamics(MD) simulations at 5.0 and 298.15 K agree very well with the optimized ones.²⁰ The calculated oxygen-hydrogen (O-H) radial distribution functions

(RDF) for pure water system are shown in Figure 3 in Ref. 21. The first peak of the O-H RDF is due to two H atoms directly bonded to O atom in a water molecule and the second peak is due to the hydrogen-bonded H atoms of different water molecules. The O-H RDF obtained by Ojāme *et al.*¹⁷ looks reasonable even though they had a system of 32 water molecules. In their MD simulation within the Ewald summation, the real-space interactions are considered to go beyond the "minimum image convention". That is, for the pair, dipole, and Coulomb interactions it is necessary to include more neighbors in the real-space summation than just the neighbors within half of the box length. All the interactions from neighbors within a distance of up to 8 unit boxes away are summed explicitly.

The calculated O-H RDF of the OSS2 model for N=216 water²¹ is in very good agreement with that obtained by Ojāme *et al.*¹⁷ except a small discrepancy at $r = 3.5\text{--}5.5$ nm. The discrepancy is a minor problem and the excellent agreement indicates that our method to calculate the induced dipole moment at each oxygen site within the Ewald summation is valid even though our method for the Ewald summation is different from that of Ojāme *et al.*

Replacing a water molecule by OH⁻ and adjusting the length of the simulation box, a system of OH⁻ among 215 water molecules is obtained. During a long equilibration simulation the transfer of H⁺ from a water molecule to the OH⁻ is occasionally observed. The calculated O-H RDF of the OSS2 model for this system is essentially the same as those for N = 216 water system.²¹

The initial solvation pattern of OH⁻ captured by our MD simulation, before a proton transfer(PT) occurs, is very similar to the resting state of four accepted (O⁻-H⁺) and no donated HB, which is predicted by BLYP of Ref. 5. This state is the most probable configuration, since a fairly long-lived time of this 4-fold coordination, before and after a

successive PTs, has been observed, even though the lengths of the four HBs are continually fluctuated. The primary cause to a PT begins with the approach of an O to H⁺, leading to another HB by H⁺. This 5-fold coordination is also a probable state, but not so much as the above 4-fold one, since it has a less long-live time. As predicted in the HCTH trajectory of Ref. 5, OH⁻ almost always accepts four HBs in addition to donating one, leading to a saturated solvation shell, and OH⁻ is rarely solvated in such a way as to receive an additional proton, thereby preventing OH⁻ from accessing a solvation pattern that allows for PT.

Fluctuations in the second solvation shell, however, reduce the number accepted HBs from four to three in the first shell of OH⁻, resulting in the solvation pattern of OH⁻ predicted by PW91 of Ref. 5, in which the OH⁻ strongly favors three accepted hydrogen bonds(HBs) by O⁻ in addition to a fourth one by H⁺. This observation is slightly different from the scenario predicted by BLYP where the reduction in the number of the accepted HBs in the above 4-fold coordination takes place and, almost simultaneously, another HB is donated by H⁺. The other difference is the relax to the initial resting state of the 4-fold coordination after a PT by BLYP, but from our MD simulation a successive PTs is captured as shown in Figure 3.

In Figure 3(a), the OH⁻ accepts three HBs by O⁻ and donates a fourth one by H⁺, and three H⁺s are continually fluctuating near O⁻. One of three H⁺s, particularly the below one, comes near O⁻ more often than others [Fig. 3(b)]. Finally a PT is completed in Figure 3(c) and it elapsed 0.060 pico-seconds (ps) since the H⁺ comes over the middle point between two O atoms at first time [Fig. 3(b)]. The solvation pattern of OH⁻ in Figure 3(c) is the 4-fold coordination as in Figure 3(a). The distance between these two O atoms of the 4-fold coordinations before and after the first PT is 0.2806 nano-meter(nm).

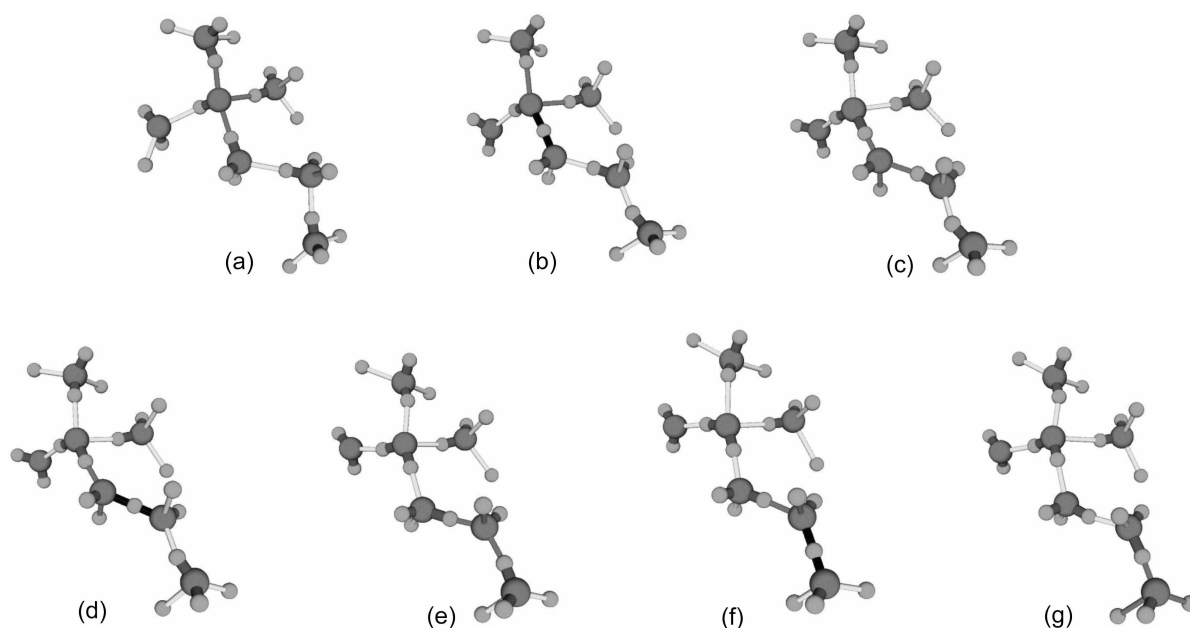


Figure 3. Snap shots of Grotthus chain mechanism captured by our MD simulation.

This 4-fold coordination structure stands 0.048 ps with minor O^{*}-H⁺ distance fluctuations before the first approach of one of three H⁺ near O^{*} for the second PT [Fig. 3(d)]. After 0.026 ps, the second PT is completed as shown Figure 3(e), and the distance between O^{*}s in Figure 3(a) and 3(e) is 0.4279 nm. After 0.024 ps the first approach occurs [Fig. 3(f)] and the third PT is completed within 0.022 ps since then [Fig. 3(g)]. The distance between O^{*}s in Figure 3(a) and 3(g) is 0.5759 nm, the time interval before and after these three PT is 0.180 ps, and the diffusion coefficient of OH⁻ is from the square displacement through the Grotthus chain mechanism is $0.307 \text{ nm}^2/\text{ps} = 3.07 \times 10^{-3} \text{ cm}^2/\text{s}$, which is an astonishingly large value when compared self-diffusion coefficient of pure water, $2.26 \times 10^{-5} \text{ cm}^2/\text{s}$ at 298 K.

After the completion of three PTs, the 4-fold coordination, three accepted HBs by O^{*} in addition to a fourth one by H⁺, cannot stand any longer: the fourth HB by H⁺ breaks down and one of the two Hs covalent-bonded to the O, which was hydrogen-bonded by the H⁺, makes the fourth accepted HB by O^{*}. Hence, the final solvation pattern of OH⁻ after three PTs is the same as the initial one - the resting state of four accepted (O^{*}-H⁺) and no donated HB.

The same kind of successive PTs has been observed after about 30 ps. In summary, four PTs occurs within 0.340 ps, the displacement is 0.7423 nm, and the calculated diffusion coefficient of OH⁻ from the square displacement through the Grotthus chain mechanism is $0.270 \text{ nm}^2/\text{ps} = 2.70 \times 10^{-3} \text{ cm}^2/\text{s}$. In the third successive PTs after about 25 ps, three PTs occurs within 0.204 ps, the displacement is 0.6209 nm, and the calculated diffusion coefficient of OH⁻ is $0.315 \text{ nm}^2/\text{ps} = 3.15 \times 10^{-3} \text{ cm}^2/\text{s}$.

In summary, successive PTs were observed three times in our MD simulation with each displacement of 0.576, 0.742, and 0.621 nm during 0.180, 0.340 and 0.204 ps, respectively. The intervals between two successive movements were about 30 and 25 ps. The average displacement in the average interval of 27.5 ps is 0.646 nm. The contribution of this Grotthus chain mechanism to the diffusion coefficient of the OH⁻ ion is estimated as $2.53 \times 10^{-3} \text{ nm}^2/\text{ps} = 2.53 \times 10^{-5} \text{ cm}^2/\text{s}$ which gives a total diffusion coefficient of $4.79 \times 10^{-5} \text{ cm}^2/\text{s}$, by adding the diffusion coefficient ($2.26 \times 10^{-5} \text{ cm}^2/\text{s}$) of bulk water at 298.15 K. Using the Einstein relationship ($u_i = D_i z_i F/RT$, u_i : ionic mobility, D_i : diffusion coefficient, and F : Faraday constant) and $\lambda_i = u_i z_i F$ (λ_i : limiting molar conductance), this value of diffusion coefficient corresponds to $\lambda_i = 180 \text{ S}\cdot\text{cm}^2/\text{mol}$ which is very close to the experimental value of limiting molar conductance of the OH⁻ ion ($\lambda = 199.1 \text{ S}\cdot\text{cm}^2/\text{mol}$) at 298.15 K.

In the previous study of Tuckerman *et al.*,⁵ the scenario captured by PW91 predicts a continuous PTs resulting in much faster of OH⁻ structural diffusion than H⁺, while that by HCTH predicts a vehicle or hydrodynamic mechanism leading to a slightly slower than water self-diffusion. On the other hand, the BLYP trajectory predicts a relax to the resting state after a PT and its occasional occurrences yielding a displacement vs time that is slower than H⁺(aq) but much faster than pure water in agreement with experiment.

However, the structural diffusion of OH⁻ captured by our MD simulation does not agree with any of these scenarios - several successive 3-4 PTs with a long time interval.

Conclusion

Molecular dynamics (MD) simulations for the system of 215 water including OH⁻ ion using the OSS2 model at 298.15 K with the use of Ewald summation was carried out. The calculated O-H radial distribution function for the system is in very good agreement with that obtained by Ojāme *et al.* A long-time MD simulation for this system revealed a successive proton transfers (PTs) from a neighbored water to the OH⁻ ion which resulted in a successive movement of OH⁻. The initial solvation pattern of OH⁻ captured by our MD simulation is a resting state of four accepted (O^{*}-H⁺) and no donated HB. This state is the most probable configuration, since a fairly long-lived time of this 4-fold coordination with fluctuation of the lengths of the four HBs have been observed. The primary cause to a PT begins with the approach of an O to H⁺, leading to another HB by H⁺. This 5-fold coordination is also a probable state with a less long-live time. Fluctuations in the second solvation shell, however, reduce the number accepted HBs from four to three in the first shell of OH⁻, in which the OH⁻ strongly favors three accepted HBs by O^{*} in addition to a fourth one by H⁺. The next step for the first PT is that one of three H⁺s comes near O^{*} more often than others and then a PT is completed. The solvation pattern of OH⁻ after the first PT is the 4-fold coordination as before. The second and third PTs occur in the same pattern and finally to finish the successive PTs, the fourth HB by H⁺ breaks down and one of the two Hs covalent-bonded to the O, which was hydrogen-bonded by the H⁺, makes the fourth accepted HB by O^{*}. Hence, the final solvation pattern of OH⁻ after successive PTs is the same as the initial one - the resting state of four accepted (O^{*}-H⁺) and no donated HB.

This is the manifestation of the Grotthus chain mechanism for the ionic mobility of the OH⁻ ion. This movement was composed of 3-4 successive PTs. This kind of successive PTs were observed three times in our MD simulation with each displacement of 0.576, 0.742, and 0.621 nm during 0.180, 0.340 and 0.204 ps, respectively, and the intervals between two successive movements were about 30 and 25 ps. The average displacement in the average interval of 27.5 ps is 0.646 nm. The contribution of this Grotthus chain mechanism to the diffusion coefficient of the OH⁻ ion is estimated as $2.53 \times 10^{-3} \text{ nm}^2/\text{ps} = 2.53 \times 10^{-5} \text{ cm}^2/\text{s}$ which gives a total diffusion coefficient of $4.79 \times 10^{-5} \text{ cm}^2/\text{s}$, by adding the diffusion coefficient ($2.26 \times 10^{-5} \text{ cm}^2/\text{s}$) of bulk water at 298.15 K. Using the Einstein relationship ($u_i = D_i z_i F/RT$) and $\lambda_i = u_i z_i F$, this value of diffusion coefficient corresponds to $\lambda_i = 180 \text{ S}\cdot\text{cm}^2/\text{mol}$ which is very close to the experimental value of limiting molar conductance of the OH⁻ ion ($\lambda = 199 \text{ S}\cdot\text{cm}^2/\text{mol}$) at 298.15 K. In conclusion, the Grotthus chain mechanism for the ionic mobility of the OH⁻ ion was reproduced by our MD simulation and the estimated limiting

molar conductance of the OH⁻ ion by this mechanism is in good agreement with the experimental value.

Acknowledgement. This work was supported by the Korea Research Foundation Grant (KRF-2003-015-C00258), in which main calculations were performed by using the supercomputing resources of the Korea Institute of Science and Technology Information (KISTI).

References

1. Zimmerman, G. H.; Gruszkiewicz, M. S.; Wood, R. H. *J. Phys. Chem.* **1995**, *99*, 11612.
 2. Ho, P. C.; Palmer, D. A. *J. Solution Chem.* **1996**, *25*, 711.
 3. Lee, S. H.; Cummings, P. T.; Simonson, J. M.; Mesmer, R. E. *Chem. Phys. Lett.* **1998**, *293*, 289.
 4. Lee, S. H.; Cummings, P. T. *J. Chem. Phys.* **2000**, *112*, 864.
 5. Tuckerman, M. E.; Chandra, A.; Marx, D. *Acc. Chem. Res.* **2006**, *39*, 151.
 6. Tuckerman, M. E.; Marx, D.; Parrinello, M. *Nature(London)* **2002**, *417*, 925.
 7. Zhu, Z. W.; Tuckerman, M. E. *J. Phys. Chem. B* **2002**, *106*, 8009.
 8. Asthagiri, D.; Pratt, L. R.; Kress, J. D.; Gomez, M. A. *Proc. Natl. Acad. Sci.* **2004**, *101*, 7229.
 9. Stillinger, F. H.; David, C. W. *J. Chem. Phys.* **1978**, *69*, 1473; **1980**, *73*, 3384; Stillinger, F. H.; Weber, T. A. *Chem. Phys. Lett.* **1981**, *79*, 259; Weber, T. A.; Stillinger, F. H. *J. Phys. Chem.* **1982**, *86*, 1314; *J. Chem. Phys.* **1982**, *76*, 4028; **1982**, *77*, 4150.
 10. Ojāme, L.; Shavitt, I.; Singer, S. J. *J. Chem. Phys.* **1998**, *109*, 5547.
 11. Singer, S. J.; McDonald, S.; Ojāme, L. *J. Chem. Phys.* **2000**, *112*, 710.
 12. Lee, S. H. *Mol. Sim.* **2003**, *29*, 211.
 13. Dang, L. X.; Smith, D. E. *J. Chem. Phys.* **1993**, *99*, 6950.
 14. Smith, D. E.; Dang, L. X. *J. Chem. Phys.* **1994**, *100*, 3757.
 15. de Leeuw, S. W.; Perram, J. W.; Smith, E. R. *Proc. R. Soc. London* **1980**, *A373*, 27.
 16. Anastasiou, N.; Fincham, D. *Comput. Phys. Commun.* **1982**, *25*, 159.
 17. Private communication to Ojāme, L.
 18. Gauss, K. F. *J. Reine Angew. Math.* **1829**, *IV*, 232.
 19. Gear, W. C. *Numerical Initial Value Problems in Ordinary Differential Equations*; Prentice-hall: Englewood Cliffs, NJ, 1971.
 20. Lee, S. H. *Bull. Korean Chem. Soc.* **2002**, *23*, 107.
 21. Lee, S. H. *Bull. Korean Chem. Soc.* **2001**, *22*, 847.
-